DOUBLE-COUPLE FAULTING MECHANISMS OF THREE LOW-FREQUENCY MARSQUAKES SUGGEST THEIR VOLCANO-TECTONIC ORIGIN

Maddy Sita[1], Victor Agaba[2] & Suzan van der Lee[2]

[1] University of Maryland, [2] Northwestern University

S0235b UTC2019-07-26T12:19:19

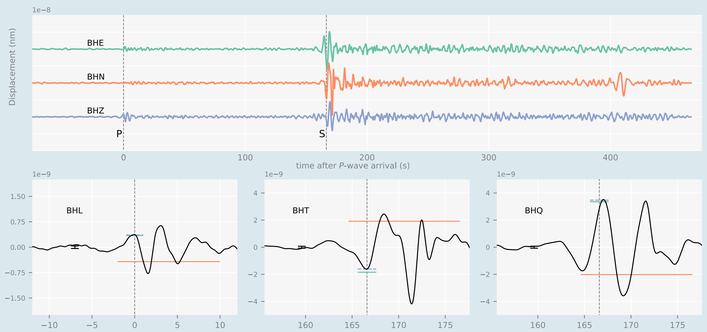

S0173a & S0173ab UTC2019-05-23T02:22:59

S0325ab UTC2019-10-26T06:59:08

Figure 1. Rotated seismograms for each event are plotted relative to the arrival of the *P*-wave at time 0. The *P*- and *S*-wave arrival times are indicated by a vertical line and horizontal lines represent the synthetic amplitudes of the *P*, *SH*, and *SV* on the L, T and Q components.

Investigating possible double-couple mechanisms

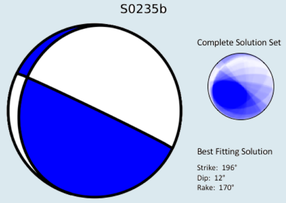

Figure 2. S0173a begins at 0 seconds and the *P*- and *S*-wave arrival for S0173ab is at 4 seconds. The back azimuth angle shifts from 90° to 86°.

The beachballs to the left show $\overrightarrow{A_s}$ that produce the smallest misfit ζ to $\overrightarrow{A_o}$ and are favored.

Exploring the doublet Marsquake event

We looked at the particle motion caused by the arrival of the *P* and *S* wave and found an apparent "movement" of the back azimuth angle over the time window indicating two events. The doublet events, S0173a and S0173ab, occurring in quick succession at similar locations and with different mechanisms could be due to a magma intrusion, as the start, propagation, and stalling of a dike intrusion creates changes in the stress field with potential to generate earthquakes[1,2].

An analysis by Sun and Tkalčić (2022) found many marsquakes in the area of Cerberus Fossae, many of whom contain similar waveforms to S0173a. Based on this repetitive nature of the seismicity, they concluded that a magmatic origin was the most likely explanation.

We propose that these diverse faulting mechanisms represent volcano-tectonic quakes resulting from deformation related to magmatic activity, including possible dike propagation or sill formation in the lower crust[3].

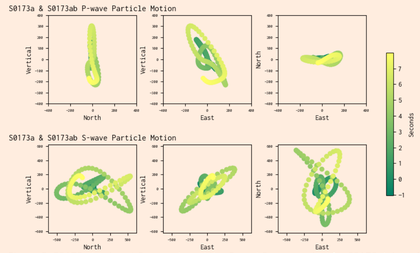

Figure 2. S0173a begins at 0 seconds and the *P*- and *S*-wave arrival for S0173ab is at 4 seconds. The back azimuth angle shifts from 90° to 86°.

Composite Mechanism

The two input mechanisms were estimated from the amplitudes of the two sets of direct body waves that arrived 4*s* apart, with identical S–P differential travel times. These two mechanisms potentially mark the sudden beginning and sudden end of a 4*s* long event, or are brittle side effects of a more prolonged, non-seismic event such as magmatic activity.

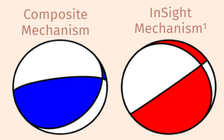

Figure 2. S0173a begins at 0 seconds and the *P*- and *S*-wave arrival for S0173ab is at 4 seconds. The back azimuth angle shifts from 90° to 86°.

Stable misfit definition for relative amplitudes

We ran forward models for each preferred mechanism to produce synthetic amplitudes for comparison to the observed amplitudes using our geometric misfit function.[2] This method involved arranging both measured and modeled P, *SV*, and *SH* amplitudes in 3D vectors that can easily be compared via their dot product, which quantifies how similar the vectors are.

Geometric Misfit

The misfit value is defined as the angle, ζ, between the two vectors, $\overrightarrow{A_s}$ and $\overrightarrow{A_o}$. Using the radius of the approximate error circle based on estimated observational error, an angle of tolerance, ε, is estimated which outlines a cone around $\overrightarrow{A_o}$.

This misfit is a smooth, intuitive function and remains stable when an amplitude vanishes. It also takes the signs (polarities) smoothly into account.

$$\epsilon = \arctan\left(\frac{e}{\|A_o\|}\right)$$

$$\zeta = \arccos\left(\frac{\overrightarrow{A_o} \cdot \overrightarrow{A_s}}{\|A_o\| \, \|A_s\|}\right)$$

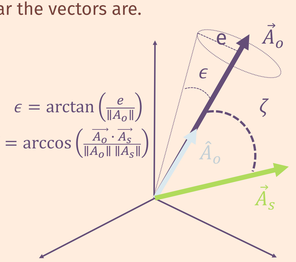

Propagating uncertainties into the grid search

Using a modified version of the Gudkova model[3] and an estimated source depth of 35km, the SV, SH and P amplitudes that resulted from a range of double-couple focal mechanisms can be generated. The calculated amplitude vector ($\overrightarrow{A_s}$) that best fits the observed amplitude vector ($\overrightarrow{A_o}$), is the one with the smallest angle (ζ) or the largest normalized dot product, to the observed vector, regardless of the vectors length. This approach is robust and effective for modeling relative amplitudes.

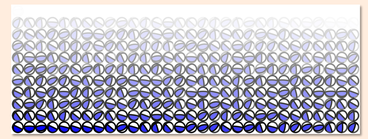

Figure 2. S0173a begins at 0 seconds and the *P*- and *S*-wave arrival for S0173ab is at 4 seconds. The back azimuth angle shifts from 90° to 86°.

Error Ellipsoids

Error estimates for observed amplitudes, inferred from noise levels, translate to an error ellipsoid in amplitude space, which converts to a set of focal mechanisms that predict the observed amplitudes within these error bounds. Only green modeled vectors are deemed acceptable matches, as they or their extensions traverse the error ellipsoid. Red vectors miss the ellipsoid and are discarded. Because noise levels differ for P, SV, and SH phases, the error ellipsoid produces a different tolerance angle for different modeled amplitude vectors.

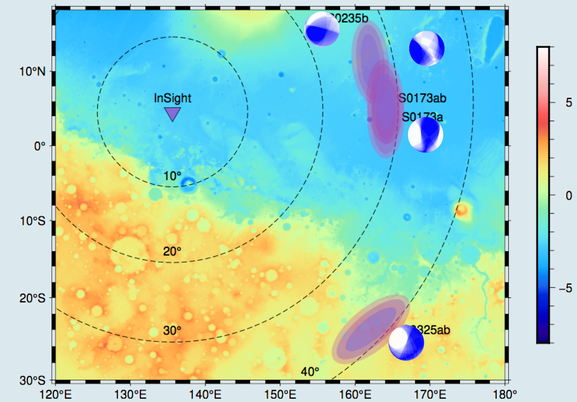

Figure 3. The figure includes S0173a, S0173ab, S0235b and the new event S0325a at an approximate latitude and longitude of ~15°N, 168°E in addition to their possible faulting mechanisms.

Conclusions

- ✓ Diversity of epicenters and fault plane solutions suggest a range of processes might be operational in the Martian lithosphere
- ✓ A likely explanation for the diversity is that the events are a result of changing stresses due to migrating magma in the lower crust, including magma dikes
- ✓ Our method presents a robust way to estimate focal mechanism from body-wave amplitudes at a single seismic station without the need for the exact planetary structure between the quake and station
- ✓ Potential applications include sparsely instrumented regions and small quakes without surface waves

This material is based upon work supported by the National Science Foundation under Grant No. AST-1757792, a Research Experiences for Undergraduates (REU) grant awarded to CIERA at Northwestern University. Any opinions, findings, and conclusions or recommendations expressed in this material are those of the author(s) and do not necessarily reflect the views of the National Science Foundation.

2. Lognonné, P., Banerdt, W.B., Giardini, D. et al. SEIS: Insight's Seismic Experiment for Internal Structure of Mars. Space Sci Rev 215, 12 (2019). https://doi.org/10.1007/s11214-018-0574-6

1. Brinkman, N., Stähler, S. C., Giardini, D., Schmelzbach, C., Khan, A., Jacob, A., et al. (2021). First focal mechanisms of Marsquakes. *Journal of Geophysical Research: Planets*, 126, e2020JE006546.

3. Banerdt, W.B., Smrekar, S.E., Banfield, D. et al. Initial results from the InSight mission on Mars. Nat. Geosci. 13, 183–189 (2020). https://doi.org/10.1038/s41561-020-0544-y

4. Taylor, J., Teanby, N. A., and Wookey, J. (2013), Estimates of seismic activity in the Cerberus Fossae region of Mars, J. Geophys. Res. Planets, 118, 2570– 2581, doi:10.1002/2013JE004469.

5. Giardini, D., Lognonné, P., Banerdt, W.B. et al. The seismicity of Mars. Nat. Geosci. 13, 205–212 (2020).

6. Zharkov, V.N., Gudkova, T.V. Construction of Martian Interior Model. Sol Syst Res **39**, 343–373 (2005). https://doi.org/10.1007/s11208-005-0049-7

UNIVERSITY OF MARYLAND · NSF · NORTHWESTERN UNIVERSITY · Northwestern CIERA CENTER FOR INTERDISCIPLINARY EXPLORATION AND RESEARCH IN ASTROPHYSICS